Selective conversion of methane to C_2 hydrocarbons using carbon dioxide over Mn–$SrCO_3$ catalysts

Yingchun Cai, Lingjun Chou, Shuben Li*, Bing Zhang, and Jun Zhao
State Key Laboratory for Oxo Synthesis and Selective Oxidation, Lanzhou Institute of Chemical Physics,
Chinese Academy of Sciences, Lanzhou 730000, China

Received 29 August 2002; accepted 3 December 2002

The combination of Mn with $SrCO_3$ leads to effective catalysts for the selective conversion of CH_4 to C_2 hydrocarbons using CO_2 as an oxidant; C_2 selectivities approach 88 and 79.1% with a C_2 yield of 4.3 and 4.5% over catalysts with an Mn/Sr ratio of 0.1 and 0.2, respectively. It is assumed that the Mn^{3+}/Mn^{2+} couple formed in the reaction plays an important role in the activation of CO_2 and CH_4.

KEY WORDS: methane; carbon dioxide oxidant; Mn–$SrCO_3$ catalysts.

1. Introduction

Recently, increasing attention has been paid on the conversion of natural gas using CO_2 as an oxidant [1]. It is well known that natural gas in many areas contains CO_2 in large quantity in addition to CH_4 and other lower alkanes. It would be highly desirable to utilize such low-valued natural gas without emission of CO_2 and convert CH_4 and CO_2 into valuable chemicals or fuels simultaneously. Unlike oxidative coupling of methane using O_2 as an oxidant, in the reaction of CH_4 with CO_2 to produce C_2 hydrocarbons, CO_2 will not induce gas-phase radical reactions, so this reaction will mainly be controlled by heterogeneous catalysis. Equilibrium conversions of CH_4 to C_2H_6 and C_2H_4 in this process were evaluated by Wang *et al.* and the results showed that yields of C_2H_6 and C_2H_4 exceed 15 and 25%, respectively, under suitable reaction conditions [2]. The key point for realization is to develop an efficient catalyst. A series of binary oxide catalysts, such as CaO–CeO_2 [2], CaO–ZnO [3], Ca–Cr_2O_3 [4] and La_2O_3–ZnO [5] were found to be effective for this reaction. Unfortunately, there are very few reports on Mn-containing catalysts, although Mn is one of the most extensively studied components in oxidative coupling of methane [6]. Recently, a series of Mn-based binary oxide catalysts were developed by Wang and Ohtsuka [7], but the catalytic performance was not satisfactory. This work was focused on the development of a more effective catalyst system for C_2 formation from CH_4 and CO_2. A novel catalyst system, Mn–$SrCO_3$, was developed on the basis of our previous work [8].

2. Experimental

Catalysts with different Mn/Sr ratios were prepared by simultaneously adding solutions with appropriate concentrations of $Mn(NO_3)_2$ (AR), and $Sr(NO_3)_2$ to 1.1 times its stoichiometric requirement of a well stirred 0.5 M aqueous solution of K_2CO_3 maintained at 70 °C. The slurry (pH $\approx$ 7.0) was filtered and then washed several times with distilled water. The resultant material was dried at 110 °C overnight and then calcined at 850–900 °C for 4–6 h. The calcined catalysts was crushed and sieved to 20–40 mesh.

X-ray diffraction (XRD) was performed on a D-MAX-RB diffractometer at 50 kV and 60 mA. The radiation source was CuKα with an Ni filter. XPS analysis of the catalysts was performed with a VG Escalab 210 spectrometer. An Mg target was used as the anode of the X-ray source with a power of 300 W. The background pressure in the detector chamber was less than 4.5×10^{-11} mbar. The pass energy of the analyzer was 30 eV in step increments of 0.06 eV. The binding energies were calibrated using the C 1s line as the reference. Near-surface compositions were calculated from peak areas using sensitivity factors, which were provided in the software of the instrument. The CO_2 TPD technique was carried out on an AM-100 instrument on Mn–$SrCO_3$ catalyst with an Mn/Sr ratio of 0.2. Before TPD measurements, the reaction of CH_4 and CO_2 under partial pressures of 30.3 kPa CH_4 and 70.7 kPa CO_2 was carried out at 875 °C for 3 h, followed by quenching to room temperature and then replacing the feed gas with He at room temperature. The TPD run was then performed at a heating rate of 10 °C/min up to 950 °C.

The reaction was performed using a conventional fixed-bed Y-type quartz reactor operated at atmospheric pressure. The inner diameter of the reactor was 9.5 mm.

---

* To whom correspondence should be addressed.

1011-372X/03/0300-0191/0 © 2003 Plenum Publishing Corporation

A 3.0 g amount of the catalyst was first loaded in the reactor and then calcined again with air (100 ml/min) at 875 °C for 1 h, followed by purging with N_2 ($\geq$99.999%, 100 ml/min) for 1 h. Finally, a mixture of CH_4 ($\geq$99.999%) and CO_2 ($\geq$99.999%) was introduced into the reactor. Unless otherwise described, the reaction temperature was 875 °C and the partial pressures of CH_4 and CO_2, denoted $P(CH_4)$ and $P(CO_2)$, were 30.3 and 70.7 kPa, respectively. After removal of H_2O, the effluent gas was analyzed using an on-line high-speed gas chromatograph. A molecular sieve 5A column was used for the analysis of H_2, CH_4, CO and CO_2; CH_4, C_2H_6 and C_2H_4 were analyzed simultaneously with a Porapak Q column. The following overall reactions were taken into account for data processing:

$$2CH_4 + CO_2 = C_2H_6 + CO + H_2O \tag{1}$$

$$2CH_4 + 2CO_2 = C_2H_4 + 2CO + 2H_2O \tag{2}$$

$$CH_4 + 3CO_2 = 4CO + 2H_2O \tag{3}$$

$$CH_4 + CO_2 = 2CO + 2H_2. \tag{4}$$

The data processing method has been described elsewhere [4].

3. Results and discussion

3.1. Effect of catalyst composition on catalytic performance

Table 1 shows the effect of the Mn/Sr ratio in the catalyst on the performance at 875 °C. As can be seen, $SrCO_3$ alone showed no obvious catalytic effectiveness for the reaction, only 0.2% CH_4 conversion was detected; on the other hand, MnO_2 alone exhibited a high CH_4 conversion of 9.8%, but the C_2 selectivity was low, only 6.3%, thus the C_2 yield was very low over MnO_2 alone. For Mn–$SrCO_3$ catalysts, the CH_4 conversion decreased to some extent compared with that of MnO_2, but the C_2 selectivity and C_2 yield increased dramatically. With Mn content increasing and Sr content decreasing, the CH_4 conversion increased and C_2 selectivity decreased. CH_4 conversion, C_2 selectivity and C_2 yield were 5.7, 79.1 and 4.5%, respectively, at an Mn/Sr ratio of 0.2. It should be pointed out that not only the C_2 selectivity but also the C_2 yield for the Mn–$SrCO_3$ catalysts is higher than that for each component. It is therefore evident that a synergy effect in C_2 formation exists between the two components. The catalyst with an Mn/Sr ratio of 0.2 was investigated in detail since it exhibited the highest C_2 yield.

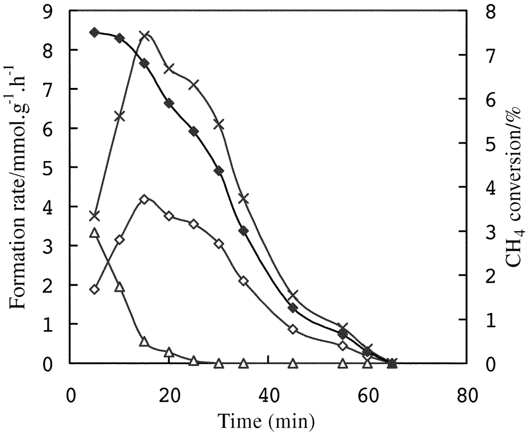

Figure 1. Reaction of CH_4 in the absence of CO_2 over the Mn–$SrCO_3$ catalyst. (◆) CH_4 conversion; (◇) formation rate of CO; (×) formation rate of H_2; (△) formation rate of CO_2.

3.2. Role of CO_2 in the conversion of CH_4 to C_2 hydrocarbons

To clarify the role of CO_2, the reactions of CH_4 over the Mn–$SrCO_3$ catalyst in the absence and presence of CO_2 were compared. In the absence of CO_2 (figure 1), the CH_4 conversion was 7.5% in the initial stage, and CO_2 and H_2O were formed at an early stage. After 20 min, only CO and H_2 were detected, the CH_4 conversion decreased abruptly with time on-stream; after about 65 min the reaction almost stopped and CO and H_2 were no longer produced. During the whole process, no C_2 hydrocarbons were detected. The reaction without CO_2 must arise from lattice oxygen atoms in the catalyst.

Table 1
Effect of catalyst composition on catalytic performance

Catalyst	CH_4 conversion (%)	CO_2 conversion (%)	C_2H_4 selectivity (%)	C_2H_6 selectivity (%)	C_2 yield (%)
$SrCO_3$	0.2	0.1	0	0	0
Mn/Sr (0.05)	1.3	0.5	10.5	70.0	1.0
Mn/Sr (0.1)	4.9	1.8	31.6	56.3	4.3
Mn/Sr (0.2)	5.7	2.3	28.4	50.7	4.5
Mn/Sr (0.3)	6.1	2.9	24.7	42.7	4.1
Mn/Sr (0.4)	6.3	3.2	20.6	40.5	3.8
Mn/Sr (0.6)	7.1	4.3	16.3	29.1	3.2
Mn/Sr (0.8)	8.3	5.3	14.6	24.3	3.1
Mn/Sr (1.0)	8.8	6.4	10.9	13.4	2.1
MnO_2	9.8	7.1	1.1	5.2	0.6

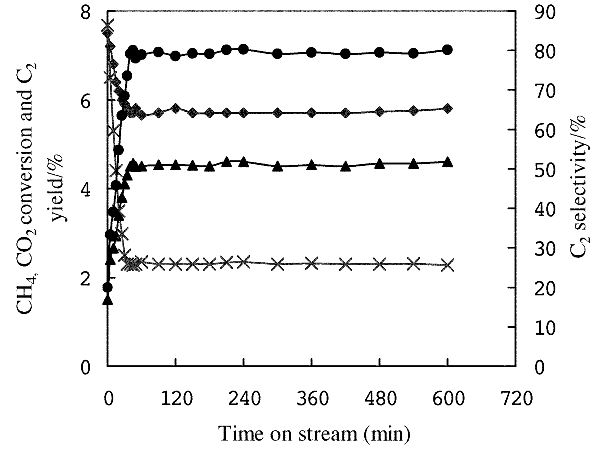

Figure 2. Change in catalytic performance of Mn–$SrCO_3$ with time on-stream. (◆) CH_4 conversion; (×) CO_2 conversion; (●) C_2 selectivity; (▲) C_2 yield.

Thus, the lattice oxygen is non-selective for C_2 formation. When CO_2 was co-fed (figure 2), a large amount of H_2O was formed during the initial 5 min; CO_2 in the effluent decreased at the same time. After 10 min, CO, C_2H_6 and C_2H_4 were detected. CH_4 and CO_2 conversion and C_2 formation reached a steady state after ~40 min; the C_2 selectivity approached about 80% with a C_2 yield of 4.5%. The results did not change even when the time on-stream was prolonged to 10 h (figure 2). The catalysts before reaction and after reaction for 1 or 10 h were subjected to XRD measurements. The results (figure 3) show that, before reaction, the crystalline phase of the catalyst was $SrCO_3$ and β-Sr_2MnO_4; after reaction of 1 h, the crystalline phase changed to $SrCO_3$, MnO and Mn_2O_3, and the crystalline phase at 1 h did not change during further reaction. The results described above indicate that the oxygen species responsible for selective C_2 formation is not from lattice oxygen, but is generated from CO_2 during the reaction.

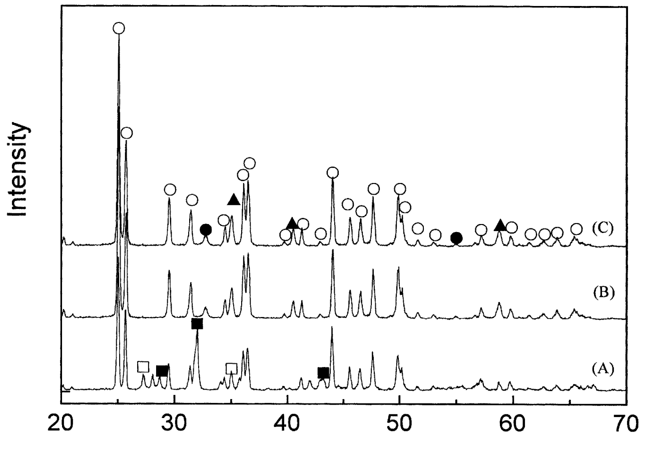

Figure 3. X-ray diffraction patterns for fresh and reacted catalysts. (A) Fresh catalyst; (B) catalyst after reaction for 1 h; (C) catalyst after reaction for 10 h. (○) $SrCO_3$; (■) β-Sr_2MnO_4; (□) $SrMnO_3$; (▲) MnO; (●) Mn_2O_3.

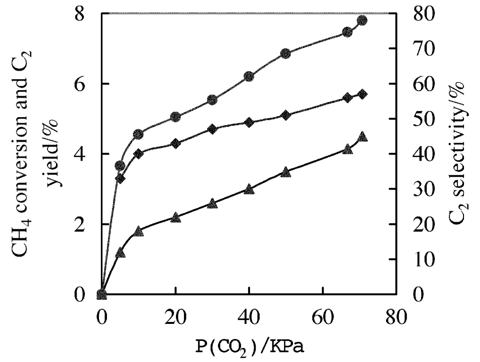

Figure 4. Catalytic activity as a function of partial pressure of CO_2 over the catalyst with an Mn/Sr ratio of 0.2. (◆) CH_4 conversion; (●) C_2 selectivity; (▲) C_2 yield.

A more detailed dependence of the performance of the Mn–$SrCO_3$ catalyst (with an Mn/Sr ratio of 0.2) on $P(CO_2)$ is plotted in figure 4. The results show that not only the C_2 selectivity but also the C_2 yield increased slightly with increase in $P(CO_2)$. It should be noted that CO_2 plays a key role in C_2 formation and achieving a high C_2 selectivity.

3.3. *Effect of reaction temperature on the performance of Mn–$SrCO_3$*

Figure 5 shows the temperature dependence of the catalytic performance at $P(CO_2)$ of 70.7 kPa. As can be seen, the CH_4 conversion and C_2 yield increased with increase in reaction temperature, and an increase in reaction temperature above 825 °C decreased the C_2 selectivity. The C_2 selectivity exceeded 90% at 825 °C and the C_2 yield reached 4.5% at 875 °C with a C_2 selectivity of 79.1%. At 900 °C, the C_2 yield was a maximum of 5.1% with a C_2 selectivity of 68.1%. Although these values are still insufficient from a practical point of view, the observed yield is one of the best results among a series of results recently reported.

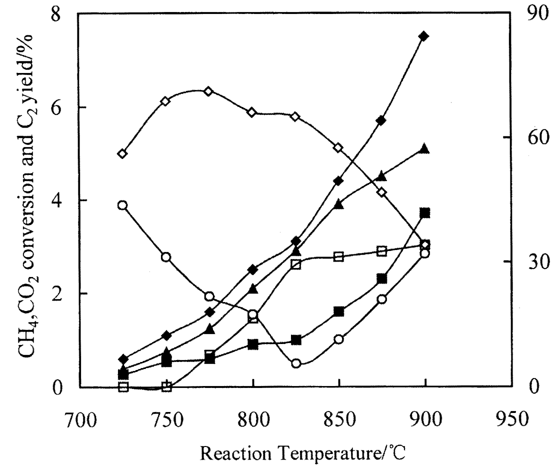

Figure 5. Effect of temperature on catalytic performance of Mn–$SrCO_3$. (◆) CH_4 conversion; (■) CO_2 conversion; (▲) C_2 yield; (□) C_2H_4 selectivity; (◇) C_2H_6 selectivity; (○) CO selectivity.

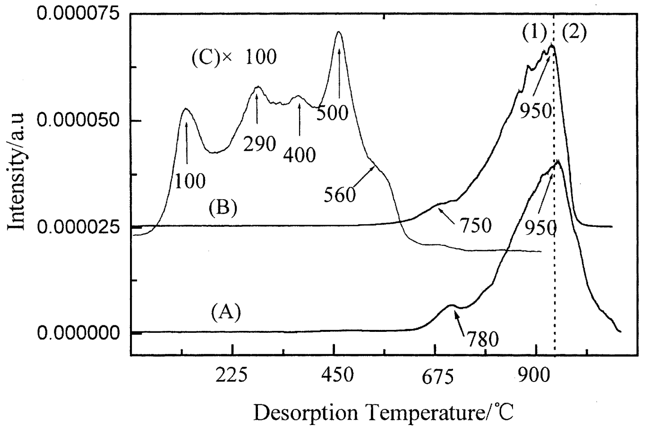

Figure 6. Profiles of CO_2 desorption from the catalysts after reaction. (A) $SrCO_3$; (B) Mn–$SrCO_3$; (C) MnO_2. Region (1), temperature increased with time; region (2), temperature decreased.

3.4. Characterization of the Mn–$SrCO_3$ catalyst after reaction

In order to explain the above phenomena and deduce the possible mechanism over Mn–$SrCO_3$ catalyst, CO_2 TPD, XRD and XPS studies were carried out.

To examine the chemisorption of CO_2 on the Mn–$SrCO_3$ catalyst after reaction, CO_2 TPD measurements were performed. Figure 6 shows the TPD results in an He flow. Two desorption peaks were observed in the case of Mn–$SrCO_3$ catalyst. The peak temperature of one was 750 °C, and the other peak increased with the increase in desorption temperature even up to 950 °C. These results may partly explain the facts that the reaction of CH_4 and CO_2 to produce C_2 hydrocarbons only takes place when the reaction temperature exceeds 750 °C and the C_2 yield increased with increase in reaction temperature. It is noteworthy that when the desorption temperature decreased after 950 °C, the desorption peak also decreased, so it is reasonable to deduce that the desorption peak of higher temperature is derived, at least partly, from the dissociation of $SrCO_3$. For comparison, CO_2 TPD was also carried out on both reacted MnO_2 and $SrCO_3$ catalysts. As shown in figure 6, the results obtained over $SrCO_3$ are very similar to those for the Mn–$SrCO_3$ catalyst. Although four CO_2 TPD peaks were observed over reacted MnO_2 catalyst, none of the peak temperature was higher than 600 °C. No CO_2 TPD peak attributable to MnO_2 was detected over Mn–$SrCO_3$ catalyst, hence the results may show that during the reaction of CH_4 and CO_2, CO_2 only desorbed on Sr sites.

The Mn–$SrCO_3$ catalyst after reaction at 875 °C under a $P(CO_2)$ of 70.7 kPa for 10 h was quenched to room temperature and instantly subjected to XRD analysis. The XRD patterns, which may be seen in figure 3, show that before reaction, $SrCO_3$ and β-Sr_2MnO_4 are the main crystalline phase, and $SrCO_3$, MnO and Mn_2O_3 were detected after reaction. Thus, bulk carbonate of Sr was formed during the reaction over the Mn–$SrCO_3$ catalyst. Based on the XRD results and the fact that a large amount of H_2O was formed at the early stage of the reaction of CH_4 and CO_2, we deduce that the following process may take place:

$$9Sr_2MnO_4 + 18CO_2 + 2CH_4 \longrightarrow 18SrCO_3 + 3MnO + 3Mn_2O_3 + 2CO + 4H_2O. \quad (5)$$

Figure 7 shows the binding energy of Mn $2p_{3/2}$ in fresh Mn–$SrCO_3$ catalyst and the catalysts after reaction times of 1 and 10 h. As shown in figure 7, the Mn $2p_{3/2}$ binding energy in the fresh Mn–$SrCO_3$ catalyst was 642.2 eV, indicating that Mn was present mainly as Mn^{4+}. The binding energy of Mn $2p_{3/2}$ shifted to 641.3

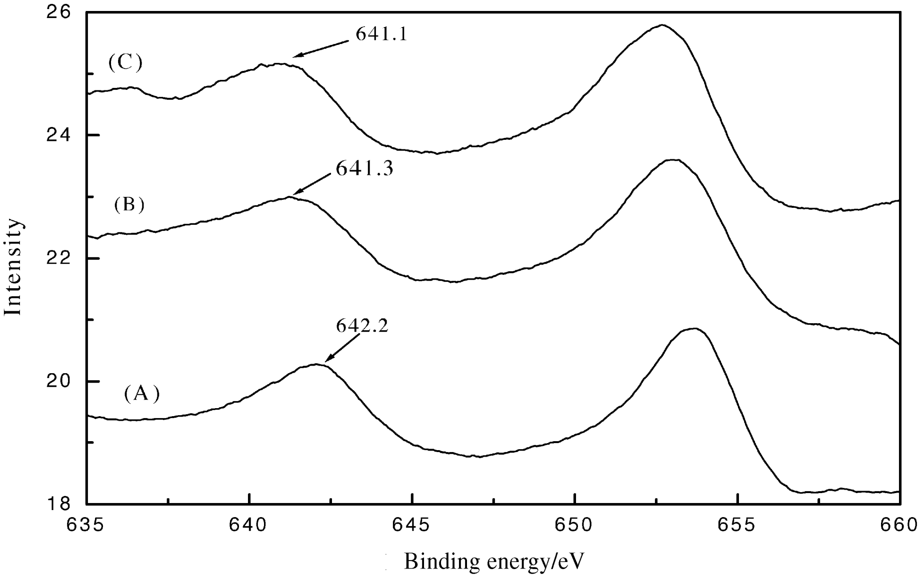

Figure 7. XPS spectra in the Mn 2p region of catalysts before and after reaction: (A) Fresh Mn–$SrCO_3$ catalyst; (B) Mn–$SrCO_3$ catalyst after reaction for 1 h; (C) Mn–$SrCO_3$ catalyst after reaction for 10 h.

Table 2
Variation of Mn/Sr atomic ratio in fresh and reacted Mn–$SrCO_3$ (Mn/Sr = 0.2) catalysts.

Catalyst	Fresh	After reaction for 1 h	After reaction for 10 h
Mn/Sr	0.22	0.089	0.084

and 641.1 eV after reaction times of 1 and 10 h, indicating that Mn^{3+} and Mn^{2+} predominated [9–11], these results are consistent with the XRD results. Table 2 lists the near-surface Mn/Sr ratios of Mn–$SrCO_3$ catalyst before and after reaction. The near-surface Mn/Sr ratio, as determined by XPS, was 0.22 before reaction and 0.089 and 0.084 after reaction times of 1 and 10 h, respectively, so during the first 1 h of the reaction of CH_4 and CO_2, Sr obviously migrated to the near-surface of the Mn–$SrCO_3$ catalyst. As time went on, the migration of Sr became insignificant, and the Mn/Sr ratio at 10 h closely approximated that at 1 h. The XPS results also show that no carbon deposit was detected on both catalysts after reaction times of 1 and 10 h. Based on the XPS results and the fact that the catalytic performance of Mn/Sr changed considerably in the first 1 h and then remained stable, we deduced that the Mn component is related to the activity of the Mn–$SrCO_3$ catalyst whereas the Sr component is related to the C_2 selectivity. In the initial stage, the Mn concentration on the surface of the Mn–$SrCO_3$ catalyst was relatively high while the Sr concentration was relatively low, so a higher CH_4 conversion and lower C_2 selectivity were obtained. As the reaction proceeded, Sr migrated to the surface of the catalyst and the Mn/Sr ratio decreased rapidly, so the CH_4 conversion decreased and C_2 selectivity increased correspondingly. After reaction for 1 h, the Mn/Sr ratio remained constant and the catalytic performance also remained stable. The results in table 1 indicating that, with increasing Mn content and decreasing Sr content, the CH_4 conversion increased but the C_2 selectivity decreased may also be attributed to the deduction that the Mn component is related to the activity whereas the Sr component is related to the C_2 selectivity.

3.5. *Possible mechanism for the reaction of CH_4 and CO_2 to produce C_2 hydrocarbons over Mn–$SrCO_3$ catalysts*

On the basis of all the above findings, the possible mechanism for CH_4 and CO_2 to produce C_2 hydrocarbons over Mn–$SrCO_3$ catalysts is as follows:

$$SrCO_3 \xrightarrow{\Delta} SrO + CO^*_{2(a)} \tag{6}$$

$$CO^*_{2(a)} + Mn^{2+} \longrightarrow Mn^{3+} + CO + O^- \tag{7}$$

$$O^- + 2CH_4 + Mn^{3+} \longrightarrow 2CH_3^{\bullet} + H_2O + Mn^{2+} \tag{8}$$

$$2CH_3^{\bullet} \longrightarrow C_2H_6 \tag{9}$$

$$C_2H_6 \longrightarrow C_2H_4 + H_2 \tag{10}$$

$$SrO + CO_2 \longrightarrow SrCO_3. \tag{11}$$

$SrCO_3$ may first dissociate at high reaction temperature to produce SrO and adsorbed $CO^*_{2(a)}$, the adsorbed $CO^*_{2(a)}$ may then be activated by reduced Mn^{2+}, CO and O^- are formed, the surface reactive oxygen species O^- on Mn–$SrCO_3$ abstract hydrogen from methane to give methyl radicals, which in turn are converted to C_2 hydrocarbons. SrO from the dissociation of $SrCO_3$ may react with carbon dioxide in the gas phase to produce $SrCO_3$ again.

On the basis of the above discussion, the reason why MnO-$SrCO_3$ is effective for the CH_4–CO_2 reaction can be attributed to both the dissociation of $SrCO_3$ to form $CO^*_{2(a)}$ and the formation of an Mn^{3+}/Mn^{2+} couple to activate $CO^*_{2(a)}$ and in turn to activate CH_4.

4. Conclusion

Mn–$SrCO_3$ catalysts are effective for the conversion of CH_4 to C_2 hydrocarbons using CO_2 as an oxidant. C_2 selectivities approach 88 and 79.1% with C_2 yields of 4.3 and 4.5% over the catalysts with Mn/Sr ratios of 0.1 and 0.2, respectively.

The possible mechanism for C_2 formation over Mn–$SrCO_3$ catalysts was deduced as follows: CO_2 dissociated from $SrCO_3$ may be activated by reduced Mn^{2+} to form active oxygen species (O^-), then O^- activates CH_4 to form $CH_3^{\bullet}$ radicals, which in turn are converted to hydrocarbons.

Acknowledgment

The authors gratefully acknowledge financial support for this work from the Ministry of Science and Technology (grant 1999022406).

References

[1] K. Asami, T. Fujita, K. Kusakabe, Y. Nishiyama and Y. Otsuka, Appl. Catal. A: Gen. 126 (1995) 245.
[2] Y. Wang, Y. Takahashi and Y. Ohtsuka, J. Catal. 186 (1999) 160.
[3] Y. Wang and Y. Ohtsuka, J. Catal. 192 (2000) 252.
[4] Y. Wang, Y. Takahashi and Y. Ohtsuka, Chem. Lett. (1998) 1209.
[5] C.L. Chen, Y.D. Xu, G.J. Lin and X.X. Guo, Catal. Lett. 42 (1996) 149.
[6] S.B. Li, Chin. J. Chem. 19(1) (2001) 16.
[7] Y. Wang and Y. Ohtsuka, Appl. Catal. A: Gen. 219 (2001) 183.
[8] Y.C. Cai, L.J. Chou, S.B. Li, B. Zhang and J. Zhao, Chem. Lett. (2002) 828.
[9] R.W. Juddy, C. Komodromos and T.J. Reyonlds, Catal. Today 13 (1992) 237.
[10] B.R. Strohmeier and D.M. Hercules, J. Phys. Chem. 88 (1984) 4922.
[11] M. Oku, K. Hirokawa and S. Ikeda, J. Electron Spectrosc. Relat. Phenom. 7 (1975) 465.